Inducing Order from Disordered Copolymers: On Demand Generation of Triblock Morphologies Including Networks

ARTICLE *in* MACROMOLECULES · JUNE 2012

Impact Factor: 5.8 · DOI: 10.1021/ma300365h

5 AUTHORS, INCLUDING:

Wei-Fan Kuan
University of Delaware
9 PUBLICATIONS **98** CITATIONS
SEE PROFILE

Benjamin S Hsiao
Stony Brook University
571 PUBLICATIONS **20,554** CITATIONS
SEE PROFILE

Thomas Epps
University of Delaware
86 PUBLICATIONS **1,751** CITATIONS
SEE PROFILE

Macromolecules

Article

pubs.acs.org/Macromolecules

Inducing Order from Disordered Copolymers: On Demand Generation of Triblock Morphologies Including Networks

Maëva S. Tureau,[†] Wei-Fan Kuan,[†] Lixia Rong,[‡] Benjamin S. Hsiao,[‡] and Thomas H. Epps, III*,[†]

[†]Department of Chemical and Biomolecular Engineering, University of Delaware, Newark, Delaware 19716, United States

[‡]Department of Chemistry, Stony Brook University, Stony Brook, New York 11794, United States

Supporting Information

ABSTRACT: Disordered block copolymers are generally impractical in nanopatterning applications due to their inability to self-assemble into well-defined nanostructures. However, inducing order in low molecular weight disordered systems permits the design of periodic structures with smaller characteristic sizes. Here, we have induced nanoscale phase separation from disordered triblock copolymer melts to form well-ordered lamellae, hexagonally packed cylinders, and a triply periodic gyroid network structure, using a copolymer/homopolymer blending approach, which incorporates constituent homopolymers into selective block domains. This versatile blending approach allows one to precisely target multiple nanostructures from a single disordered material and can be applied to a wide variety of triblock copolymer systems for nanotemplating and nanoscale separation applications requiring nanoscale feature sizes and/or high areal feature densities.

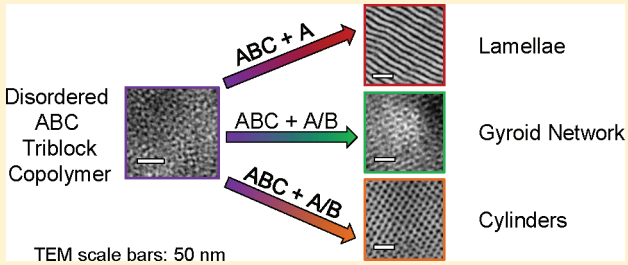

INTRODUCTION

Many emerging nanotechnology applications such as separation membranes, lithographic masks, and battery and fuel cell membranes rely on the creation of polymeric materials that self-assemble into well-ordered periodic nanostructures with minimal synthesis and processing. Block copolymers are one class of soft material, consisting of two or more covalently bonded chains of chemically distinct monomers that can be selected to match the chemical and mechanical properties needed for a particular application.[1−3] Additionally, these materials allow for the design of a variety of complex structures on nanometer length scales, including several triply periodic network structures exhibiting improved mechanical properties.[4−8] Unlike hexagonally packed cylindrical nanostructures that often require alignment techniques to minimize structural defects,[9,10] nanoscale network morphologies are particularly attractive due to their continuously percolating domains in three dimensions and short diffusion path lengths, which can facilitate transport in applications such as water filtration and ion-conduction membranes.[8,11,12]

The tendency of block copolymers to phase separate is dictated by the degree of block incompatibility and conformational entropy of the polymer chains, quantitatively described by the segregation strength (χN), which is the product of the Flory−Huggins interaction parameter between two blocks (χ) and the overall degree of polymerization (N).[13] Three segregation regimes typically characterize ordering in block copolymers: the strong segregation limit (SSL, $\chi N \geq 100$ in diblock copolymers) where sharp domain boundaries are formed with minimal interfacial mixing, the intermediate segregation regime (ISR, $\sim 10 \leq \chi N \leq 100$ in diblocks), and the weak segregation limit (WSL, $\chi N \leq 10$ in diblocks) where the copolymers are considered disordered due to the high degree of block mixing.[14,15] The critical segregation strength required to induce a transition from a disordered state to an ordered state relies on the fine control over N ($\propto M_n$, i.e. number-average molecular weight) and χ (typically $\propto 1/T$, i.e. inverse temperature). While χ depends on the volume fractions of the respective copolymer components,[13] both N and χ play a crucial role in the order-to-disorder transition (ODT) temperature of a particular copolymer system. In symmetric diblock copolymers, field-theoretic simulations−complex Langevin (FTS-CL) calculations, which include fluctuation corrections to the mean-field phase diagram by Matsen,[16] predict this order-to-disorder transition (ODT) at $\chi N_{ODT} \sim 12$.[17] In ABC triblocks, finding the critical χN_{ODT} value is complicated by the increased number of tunable parameters, including three χ-parameters (χ_{AB}, χ_{BC}, and χ_{AC}), two independent volume fractions (f_A and f_B, where $f_C = 1 - f_A - f_B$), and N ($N = N_A + N_B + N_C$). For a given system, this critical χN value can be reached by synthesizing copolymers of sufficient M_n (i.e., large enough N) to induce ordering. When the χN value is too low for phase segregation to occur, the copolymer remains in a disordered state.[18] These weakly segregated disordered systems are generally undesirable in most nanoscale applications due to their inability to form well-defined nanostructures with suitable order. However, finding ways to induce order in disordered copolymer melts of relatively low molecular weight offers

Received: February 21, 2012
Revised: May 15, 2012
Published: May 25, 2012

Table 1. Characterization Data for ISM Triblock Copolymers, Homopolymers, and Associated Blends

	homopolymer		volume composition[c]					
materials	type	f_h[b]	f_I	f_S	f_M	M_n (g mol^{-1})	PDI	phase
triblocks								
T1			0.24	0.58	0.18	19600	1.09	DIS
T2			0.16	0.57	0.27	20500	1.08	DIS
homopolymers								
PI			1.00			4400	1.16	
PS				1.00		13600	1.06	
PMMA					1.00	6000	1.13	
blends[a]								
B1-1	PMMA	0.10	0.22	0.52	0.26			DIS
B1-2	PI	0.14	0.35	0.49	0.16			LAM
B1-3	PI/PS	0.13/0.10	0.32	0.54	0.14			Q^{230}
B1-4	PI/PS	0.09/0.13	0.28	0.58	0.14			HEX
B2-1	PMMA	0.03	0.15	0.56	0.29			DIS
B2-2	PMMA	0.05	0.15	0.54	0.31			DIS
B2-3	PMMA	0.08	0.14	0.53	0.33			PL[d]
B2-4	PMMA	0.11	0.14	0.51	0.35			LAM
B2-5	PMMA	0.12	0.14	0.50	0.36			LAM
B2-6	PMMA	0.15	0.13	0.49	0.38			LAM

[a]Polymer blend names annotated as "B1-*x*" and "B2-*x*" refer to blends from parent triblocks T1 and T2, respectively. [b]Homopolymer volume fraction f_h is calculated from the ratio of homopolymer volume to total blend volume. [c]Volume compositions in polymer blends represent the overall volume fraction of each species. [d]Blend B2-3 is tentatively assigned a perforated lamellar (PL) morphology.

significant advantages. For example, low molecular weight copolymers possess higher chain mobility relative to their high molecular weight counterparts, allowing for better processability and potentially facilitating the formation of nanostructures with greater degrees of order under moderate processing conditions.[15,20] Additionally, as domain size depends primarily on molecular weight, block copolymers of lower molecular weight possess smaller domain sizes, potentially facilitating patterning in miniature electronic devices.[19]

In the past decade, considerable efforts have been made to induce ordering in otherwise disordered block copolymers by the selective incorporation of nanoparticles[21] and other additives within copolymer domains.[22,23] For example, several research groups have shown that the selective formation of salt complexes with a particular block induced order−order transitions (OOTs) or disorder−order transitions (DOTs) in block copolymers.[24−31] Similarly, Wiesner and co-workers have reported OOTs in block copolymer−ceramic hybrid materials via the addition of metal alkoxides within a particular block through a sol−gel process.[32] Additionally, Watkins and co-workers have demonstrated induced DOTs in triblock copolymers via hydrogen bonding of the constituent poly(ethylene oxide) chains with small molecule additives, such as nonconstituent homopolymers or hydrogen-bond-donating molecules.[22,33,34] Recent investigations also have reported DOTs, induced by the chemical modification of an additive blended to a disordered copolymer upon UV irradiation[23,35] or induced by alkyne/azide click chemistry in binary blends of copolymers containing alkyne functionality and azide molecules.[36,37] Although inducing order from disordered copolymers is an attractive approach toward nanoscale applications, these order-inducing methods are system specific, for instance, requiring copolymers with a block that complexes with alkali metal salts or a hydrogen-bonding block that favorably interacts with an additive. Furthermore, a more versatile order-inducing protocol with improved morphological control is necessary to facilitate the formation of highly ordered three-dimensional networks in a wider array of block copolymer systems.

Blending diblock copolymers with corresponding homopolymers is a well-established method for controlling morphology in ordered systems by adjusting block copolymer compositions.[18,38−48] Provided that relatively small homopolymer contents are used and that the molecular weights of the homopolymer and associated copolymer block are reasonably close, the phases found in diblock/homopolymer and triblock/homopolymer blends generally resemble those noted in neat composition-equivalent materials,[40] including the formation of multiply continuous network structures.[41−43,49−52] However, the addition of constituent homopolymer in the corresponding copolymer block domain can sometimes relieve packing frustration, hence enabling the stabilization of new structures such as cocontinuous phases.[43] To the best of our knowledge, however, no systematic attempt to generate multiple nanostructures by ordering a single disordered triblock using a triblock copolymer/constituent homopolymer blending approach has been reported.

Here, we present the induced ordering of two different disordered triblock copolymers via the incorporation of constituent homopolymers into particular block domains, allowing for the design of complex and ordered nanostructured materials while retaining the ease of processability provided by the disordered parent copolymers. This straightforward approach can be applied to many block copolymer systems and enables the precise targeting of a variety of nanostructures from a single, weakly segregated disordered triblock copolymer. Thus, our method alleviates the need to synthesize a new block copolymer for each desired nanostructure. Of particular significance, this blending technique allowed us to order a disordered triblock copolymer into a well-ordered network morphology, among other nanoscale structures.

EXPERIMENTAL SECTION

Material Synthesis. The poly(isoprene-*b*-styrene-*b*-methyl methacrylate) [ISM] triblock copolymers and the corresponding PI, PS, and PMMA homopolymers were synthesized under an argon atmosphere in a sealed reactor, using conventional anionic polymerization techniques. Detailed synthetic protocols can be found elsewhere.[51,53−55] The requisite PI, PS, and PMMA homopolymers were synthesized with molecular weights close to the corresponding block molecular weight of the triblock material to allow the homopolymer to localize to the corresponding block copolymer domain, without significant chain distortion.[38−41,50]

Blend Preparation. The ISM triblock/homopolymer blends were prepared by dissolving the desired homopolymer and neat triblock materials (~0.5 g total) in ~10 mL of methylene chloride, which is a good solvent for all copolymers and homopolymers. Blends of disordered ISM triblock copolymer and homopolymers were prepared with homopolymer loadings up to 23 vol %; higher homopolymer loadings were not used, as they can lead to macroscopic phase separation of the blends.[51] Typically, the blend solutions were stirred for ~12 h and were thoroughly dried under vacuum prior to analysis.

Chemical Characterization. Gel permeation chromatography (GPC) was performed on a Viscotek 270max modular system, using Waters Styragel HR1 and HR4 columns (7.8 × 300 mm each) in series, with tetrahydrofuran (THF) as the mobile phase. The number-average molecular weight (M_n) and polydispersity index (PDI) for each triblock copolymer and homopolymer were calculated based on polystyrene standards and are presented in Table 1. Proton nuclear magnetic resonance (^{1}H NMR) spectra were obtained using a Bruker AV-400 instrument. The integrated ^{1}H NMR peak intensities were used to calculate component mole fractions (for the triblock copolymers and triblock copolymer/homopolymer blends) and were converted to volume fractions using homopolymer densities at 140 °C (0.83, 0.97, and 1.13 g mL^{-1} for PI, PS, and PMMA, respectively).[56] The ^{1}H NMR spectra also were used to ensure the complete drying of the blends by monitoring the disappearance of the methylene chloride peak. Characterization data are reported in Table 1.

Small-Angle X-ray Scattering (SAXS). Most synchrotron small-angle X-ray scattering (SAXS) experiments were performed at the Advanced Photon Source (APS) of the Argonne National Laboratory on the DND-CAT beamline, using an incident beam of wavelength λ = 0.72928 Å and Mar CCD detector at a sample-to-detector distance of 6.55 m. For samples T2, B1-3, and B1-4, SAXS experiments were conducted at the National Synchrotron Light Source (NSLS) of the Brookhaven National Laboratory on the X27C beamline, using an incident beam of wavelength λ = 1.371 Å and Mar CCD detector at a sample-to-detector distance of 1.8 m. All two-dimensional scattering data were azimuthally integrated, resulting in plots of scattering intensity versus scattering vector modulus, $q = 4\pi\lambda^{-1}\sin(\theta/2)$, where θ is the scattering angle. When necessary, the SAXS patterns in this work are shifted vertically for clarity. SAXS samples were thermally annealed under vacuum and then cooled to 30 °C prior to data acquisition. The thermal annealing conditions for each sample are reported in the Supporting Information (Table S1).

Transmission Electron Microscopy (TEM). TEM micrographs were acquired on a JEOL JEM-2000FX electron microscope operating at 200 kV, with the exception of sample B1-3, which was imaged on a Tecnai-12 instrument operating at 120 kV. The annealed SAXS samples were cut on a Leica Reichart Ultracut cryo-microtome at −75 °C using a Diatome diamond knife. The specimen sections, usually 70−100 nm thick, were placed on 400 mesh copper grids and vapor-stained using a 4% aqueous OsO_4 solution for 15−20 min to improve the electron density contrast between the stained PI-domains (dark) and PS- and PMMA-domains (light).

RESULTS AND DISCUSSION

Figure 1 shows the location of the two disordered ISM materials and their associated blends, which are pertinent to this work, overlaid on the neat ISM estimated phase regions explored in previous investigations.[51] In particular, the

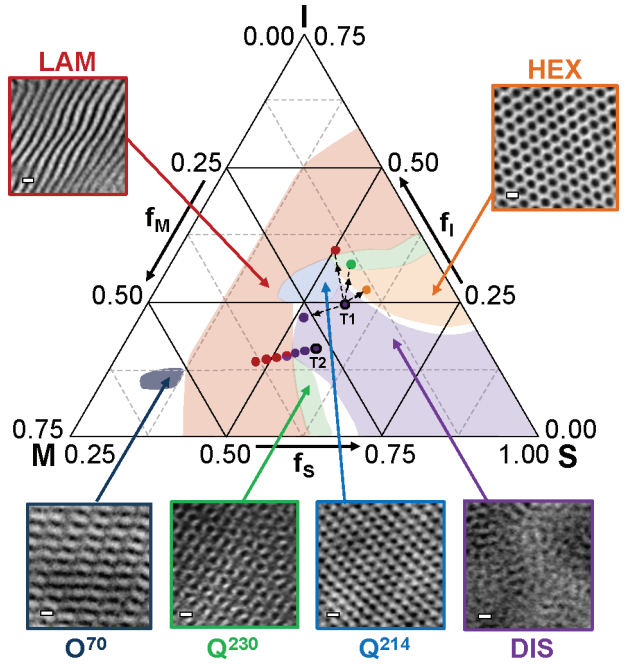

Figure 1. Locations of the two disordered ISM materials and their associated blends overlaid on the neat ISM phase map, where previously discovered phase regions of lamellae (LAM), hexagonally packed cylinders (HEX), disordered melt (DIS), and three network structures (Q^{214}, Q^{230}, and O^{70}) are colored to guide the eye.[51] The TEM micrographs show visual representations of the various nanostructures (scale bars: 20 nm). Two ISM disordered melts (T1 and T2) are represented by the purple circle. Blended specimens of triblock T1 with PI and triblock T2 with PMMA (red circle) show a DIS-to-LAM phase transition, while blends of T1 with PI and PS homopolymers at different homopolymer volume fractions show DIS-to-HEX (orange circle) and DIS-to-Q^{230} network (green circle) phase transitions. The T2/PMMA blend, represented by the mixed purple and red circle, indicates a possible perforated-lamellar (PL) phase, close to the disorder-to-order phase boundary.

disordered triblock T1 is conveniently located near a rich variety of nanostructures, which allowed for the simple, yet strategic blending of this disordered melt with judicious amounts of homopolymers to target multiple nanostructures from this single disordered triblock copolymer.

Targeting Multiple Nanostructures from a Single Disordered Triblock Copolymer. Four samples were obtained by blending the disordered ISM triblock copolymer T1 (M_n = 19.6 kg mol^{-1} and 24:58:18 vol % PI:PS:PMMA) with specific amounts of constituent homopolymers (see Table 1): Blends B1-1 and B1-2 were prepared by mixing triblock T1 with 10 vol % of PMMA and 14 vol % of PI, respectively, and blends B1-3 and B1-4 were made by mixing T1 with two homopolymers in different homopolymer amount ratios (13/10 and 9/13 vol % PI/PS, respectively). SAXS data, acquired at 30 °C for triblock T1 and associated blends (B1-1 through B1-4), are presented in Figure 2. The SAXS pattern for triblock T1 shows a broad primary peak over the entire annealing temperature range (up to 210 °C), suggestive of a disordered state morphology (DIS). Additionally, this disordered structure is supported by the TEM micrograph in Figure 3a where local ordering, shown by arrowheads, likely forms due to composition fluctuations and suggests that the effective χN parameter of triblock T1 is near the χN value for nanoscale phase separation.[18] Comparable SAXS (Figure 2) and TEM

dx.doi.org/10.1021/ma300365h | *Macromolecules* 2012, 45, 4599−4605

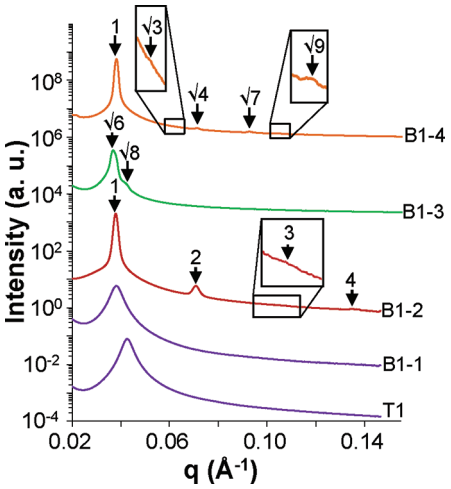

Figure 2. SAXS data acquired at 30 °C for blends associated with ISM triblock T1. From bottom to top: T1 (DIS), B1-1 (DIS), B1-2 (LAM), B1-3 (Q^{230} network), and B1-4 (HEX).

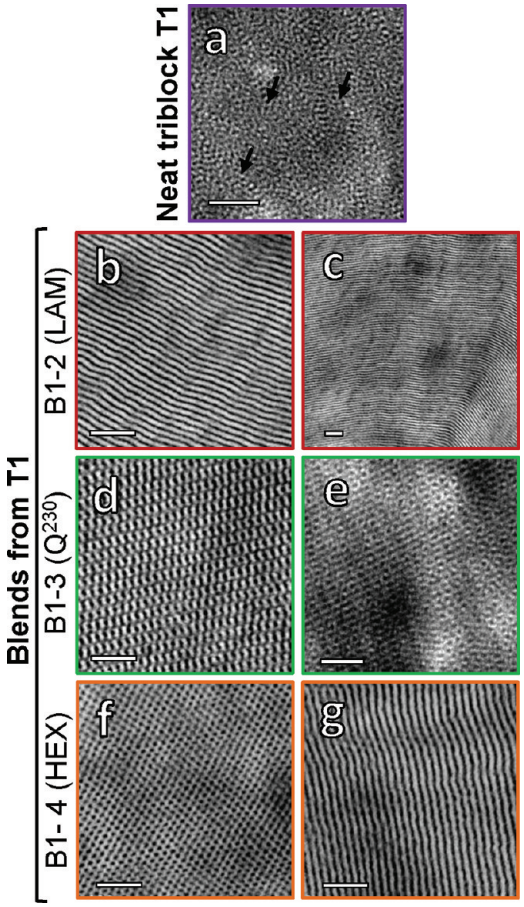

Figure 3. TEM micrographs obtained from (a) T1, (b, c) B1-2, (d, e) B1-3, and (f, g) B1-4. The TEM images are consistent with a disordered morphology (DIS) for T1 (a) for which noticeable local ordering is seen (black arrowheads),[18] a lamellar morphology (LAM) for blend B1-2 (b, c), a Q^{230} (double gyroid) network structure with two complementary [125] (d) and [111] (e) projections for B1-3, and hexagonally packed cylinders (HEX), showing perpendicular (f) and parallel (g) orientations for B1-4. Dark regions depict the OsO_4-stained PI domains, while unstained PS and PMMA domains appear lighter. Scale bars represent 100 nm.

(not shown) data to T1 are noted for blend B1-1, indicating that blend B1-1 also remains in a disordered state. Upon addition of 14 vol % PI homopolymer, blend B1-2 displays a different SAXS pattern with peak positions at q^*, $2q^*$, $3q^*$, and $4q^*$, indicative of a lamellar morphology (LAM). The near extinction of the $3q^*$ peak possibly suggests a three-domain LAM morphology.[6] The TEM micrographs for blend B1-2 in Figures 3b and 3c support the well-ordered lamellar structure assignment, where the dark layers correspond to the OsO_4-stained PI block. Blend B1-3, resulting from mixing triblock T1 with 13 vol % PI and 10 vol % PS homopolymer, exhibits a SAXS pattern with peaks at $\sqrt{6}q^*$ and $\sqrt{8}q^*$, where the primary peak is assigned to $\sqrt{6}q^*$ ($q^* = q_{112}$). Despite the absence of higher order peaks, the SAXS pattern suggests an $Ia\bar{3}d$ space group symmetry, characteristic of a double-gyroid (Q^{230}) network morphology. The corroborative TEM micrographs illustrated by the two complementary projections at lattice orientations [125] (Figure 3d) and [111] (Figure 3e) provide further evidence in support of the Q^{230} network phase assignment.[6,8] Notably, the TEM image in Figure 3e shows the well-recognizable "wagon-wheel" projection, characteristic of the Q^{230} double-gyroid network structure. Blend B1-3 is speculated to form PI channels (dark), surrounded by thick PS shells that highly mix with the minority PMMA component (light) due to the low χ_{SM} value[57] relative to χ_{IM}.[58,59] The annealing protocols for the specimens imaged in Figures 3d and 3e can be found in the Supporting Information, and we note that the sample in Figure 3e was heated above its order–disorder transition temperature (T_{ODT}) and then cooled to room temperature prior to imaging. Thus, the Q^{230} network phase is likely the stable morphology for this specimen. Lastly, blend B1-4, prepared from a blend of triblock T1 with 9 vol % PI and 13 vol % PS, produces a different SAXS signature with reflections found at q^*, $\sqrt{3}q^*$, $\sqrt{4}q^*$, $\sqrt{7}q^*$, and $\sqrt{9}q^*$, indicative of a hexagonal symmetry. The perpendicular (Figure 3f) and parallel (Figure 3g) orientations of blend B1-4, displayed in the TEM micrographs, suggest a hexagonally packed cylindrical morphology (HEX). Although OsO_4-staining does not allow us to distinguish between PS and PMMA domains, the HEX-forming blend B1-4 is expected to form PI cylinders (dark) in a matrix of PS, and highly mixed PMMA chains segregating into the PS domains, away from the PI cylinders, in agreement with the low χ_{SM} value[57] relative to χ_{IM}.[58,59] The LAM, Q^{230}, and HEX morphologies found in respective blends B1-2, B1-3, and B1-4 are consistent with the estimated phase regions of the ISM phase map[51] (see Figure 1) and also closely match the theoretical phase behavior of a comparable symmetric model ABC system of similar segregation strengths and statistical segment length ratios, calculated from self-consistent-field theory (SCFT) by Tyler et al.[60]

DIS-to-LAM Transition by Incremental Homopolymer Addition. This versatile blending technique also was applied to another DIS copolymer/homopolymer pair to show that the gradual addition of homopolymer induces a DOT, which occurs as a result of changes in the overall blend composition. In this case, a DIS triblock copolymer T2 (M_n = 20.5 kg mol^{-1} and 16:57:27 vol % PI:PS:PMMA) was blended with incremental amounts of PMMA up to 15 vol % homopolymer. The SAXS patterns of the neat DIS triblock T2 and associated blends B2-1 through B2-6, acquired at 30 °C, are provided in Figure 4. Triblock T2 was characterized as a DIS melt over the entire range of temperatures explored, as evidenced by the

dx.doi.org/10.1021/ma300365h | Macromolecules 2012, 45, 4599–4605

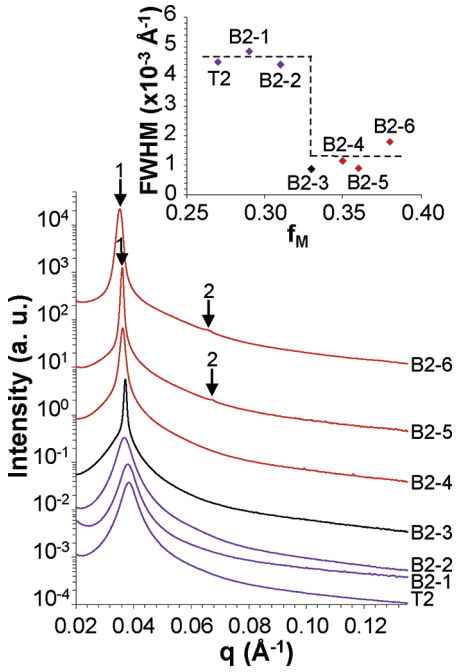

Figure 4. SAXS patterns for triblock T2, and associated blends of T2 with PMMA homopolymer (B2-1 to B2-6), acquired at 30 °C. T2 (neat ISM triblock), B2-1 (3 vol % PMMA homopolymer), and B2-2 (5 vol % PMMA homopolymer) are disordered. In blend B2-3 (8 vol % PMMA), the primary peak sharpens, indicative of a gradual ordering. A complete DIS-to-LAM phase transition occurs with addition of 11−15 vol % PMMA homopolymer in blends B2-4, B2-5, and B2-6, indicated by the narrowing of the respective primary peaks, and the appearance of a second-order peak ($2q^*$) for blends B2-5 and B2-6. As seen in the inset, the sharp narrowing of the primary peak indicated by the reduction in the full width at half-maximum (fwhm) with respect to the total PMMA volume fraction (f_M) is highly suggestive of ordering.

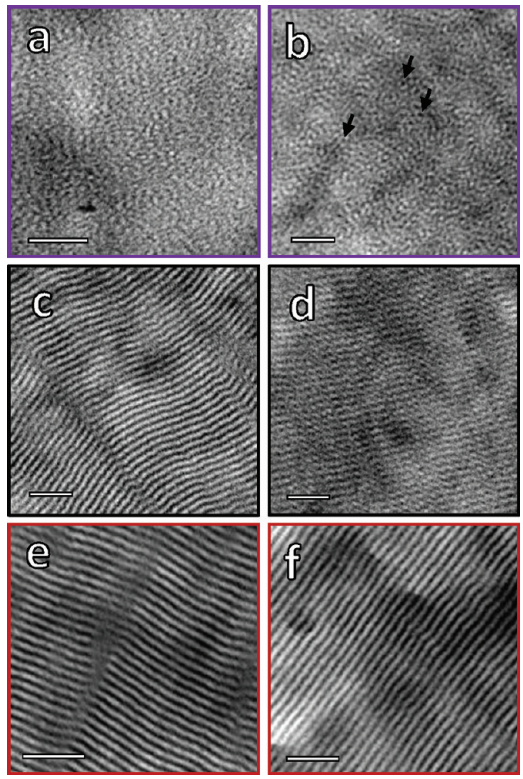

Figure 5. TEM micrographs obtained from (a) T2, (b) B2-2, (c, d) B2-3, (e) B2-4, and (f) B2-6. Blend B2-2 (b) remains in a disordered state with noticeable local ordering regions (arrowheads), indicative of the close proximity of this blend to the order−disorder phase boundary.[18] The TEM images for blend B2-3 in (c) reveals a possible perforated-lamellar (PL) morphology, more clearly illustrated in (d). The TEM projections for the blended specimens in (e) and (f) are consistent with a LAM morphology. Scale bars are 100 nm.

single broad peak in the SAXS pattern (Figure 4) and by the lack of apparent ordering (TEM image of Figure 5a). Upon the addition of 3 and 5 vol % PMMA, the respective blends B2-1 and B2-2 remained in the disordered state (Figure 4). However, in Figure 5b, the TEM image for blend B2-2 shows disorganized phase separation with noticeable locally ordered regions (shown by the arrowheads), similar to triblock T1 and to a disordered phase found in a diblock copolymer/homopolymer blend by Spontak et al.[18] Consequently, the sharper domains, revealed by the higher electron density contrast between the blocks, suggest that this blend exhibits a greater degree of phase separation in comparison to the disordered parent triblock T2 and possesses an effective χN approaching the boundary for phase separation. The homopolymer-induced ordering transition occurs at ≈8 vol % PMMA homopolymer, as seen in blend B2-3. The noticeable narrowing of the primary peak (Figure 4) confirms the gradual ordering of the blended materials upon PMMA addition, but the absence of higher order peaks suggests minimal long-range order. Additionally, the persisting broader base of the primary peak in the SAXS pattern of blend B2-3 provides evidence of possible coexistence of the ordered and disordered phases. As shown in the inset of Figure 4, the sharp drop in the full width at half-maximum (fwhm) of the SAXS primary peaks (dashed line is to guide the eye) suggests a DOT between blends B2-2 and B2-3. We note that the small fwhm variations when comparing the ordered samples to each other likely result from the slight differences in annealing conditions between the samples. (A similar note also applies to the disordered samples.) Therefore, blend B2-3 is close to the precise location at which the homopolymer-induced ordering of triblock T2 occurs. As shown in the corresponding TEM images of Figure 5c,d for blend B2-3, the lamellar layers appear periodically interconnected, suggestive of a perforated lamellar (PL) morphology.[61] These perforated lamellae (PL) nanostructures have been reported to be thermodynamically "pseudo-stable" in the pathway between DIS-to-LAM transition in blends[18] as well as between LAM-to-HEX transition[62] and LAM-to-Q^{230} network transition[63] in diblock copolymers. Further, blend B2-3 is situated near the intersection of the estimated PMMA-rich DIS, Q^{230}, and LAM phase boundaries of the ISM phase map (see Figure 1) and in the close vicinity of the HEX region predicted in the Tyler et al. ABC phase diagram.[60] Therefore, possible composition fluctuations resulting from the close proximity of blend B2-3 to the disordered-to-ordered regions along with the relief of packing frustration by the homopolymer could have stabilized a transient PL morphology in the blend.[43,64] However, upon addition of 11 vol % PMMA homopolymer, a more defined LAM morphology occurs in blend B2-4 as indicated by the TEM micrograph in Figure 5e. This blend provides the unambiguous delineation of the DIS-to-LAM phase transition between blends B2-2 and B2-4. The SAXS patterns of blends B2-5 and B2-6 show a weak second-order peak at $2q^*$, indicating increased ordering of the LAM-

dx.doi.org/10.1021/ma300365h | Macromolecules 2012, 45, 4599−4605

forming blends, which is confirmed by TEM (Figure 5f for blend B2-6). Blends B2-4, B2-5, and B2-6 show morphological consistency with the predictions of Tyler et al. model ABC phase diagram[60] as well as experimental ISM triblock copolymer materials.[51]

Factors That Influence Ordering in Disordered Triblocks. Although this induced ordering is primarily attributed to changes in the composition of the blended materials with respect to the parent triblock, the homopolymer type, homopolymer chain length, and its local distribution in the respective copolymer domain also may influence the effective segregation strength of the copolymer blend and ultimately could alter the phase boundaries of the system.[38,39,43,50] While we do not expect the end-block blending of ABC triblocks to significantly affect the conformational entropy due to the localization of A and C homopolymers to the center of the respective domains, the addition of B homopolymer to the middle-block could increase the packing frustration in the B-domain bridging the A and B chain-ends, forcing the B-chains to stretch in order to accommodate the B homopolymer.[51] In the case of Q^{230} network-forming blend B1-3 and HEX-forming blend B1-4, end-block and middle-block blending occur simultaneously. The PI and PS homopolymers have slightly differing molecular weights from the corresponding copolymer block ($M_{n,PI,h}/M_{n,PI,T1}$ = 1.09 and $M_{n,PS,h}/M_{n,PS,T1}$ = 1.19), which may induce a certain degree of polydispersity in the respective PI and PS domains of the blended materials. In this case, there may be a tendency for the PI/PS−PMMA interface to curve toward the more polydisperse PI domains, favoring the formation of the PI network channels found herein.[65]

CONCLUSIONS

In summary, a straightforward copolymer/homopolymer blending technique was exploited to induce the ordering of disordered triblock copolymers, forming a variety of nanostructures without the need for intensive synthesis to obtain each structure. The precise targeting of the blend nanostructures was rendered possible through knowledge of the composition space of ISM triblock copolymers. In addition to lamellar and hexagonally packed cylindrical morphologies, a highly ordered gyroid network structure was found using this order-induced blending method. This blended network morphology contains three-dimensional percolating nanochannels, offering improved mechanical strength while providing easier processability, and can promote transport in applications such as filtration and ion-conducting membranes. DIS-to-PL-to-LAM phase transitions also were obtained by incremental additions of PMMA homopolymer to a disordered ISM copolymer. This gradual ordering was attributed to changes in the overall blend composition and possible composition fluctuations occurring at close proximity to order−disorder phase boundaries. This versatile blending approach can be readily applied to many disordered triblock copolymers for nanoscale applications. Specifically relevant to any disordered block copolymers containing a sacrificial block such as PMMA, poly(dimethylsiloxane) (PDMS), or poly(lactide) (PLA), the gradual addition of PMMA, PDMS, or PLA homopolymer to the respective block domain also offers increased domain size tunability for the fine-tuning of pore sizes in nanoporous membranes.

ASSOCIATED CONTENT

Supporting Information

Thermal annealing conditions for the reported neat and blended ISM materials. This material is available free of charge via the Internet at http://pubs.acs.org.

AUTHOR INFORMATION

Corresponding Author

*E-mail: thepps@udel.edu.

Notes

The authors declare no competing financial interest.

ACKNOWLEDGMENTS

This work was supported by NSF-NER (CBET-0707507), NSF-CAREER (DMR-0645586), and AFOSR-PECASE (FA9550-09-1-0706). M. Tureau acknowledges an Air Products and Chemicals, Inc. Fellowship. Use of the DuPont−Northwestern−Dow Collaborative Access Team (DND-CAT) located at Sector 5 of the Advanced Photon Source (APS) was supported by E. I. DuPont de Nemours & Co., The Dow Chemical Company, and the State of Illinois. Use of the APS was supported by the U.S. Department of Energy, Office of Science, Office of Basic Energy Sciences, under Contract DE-AC02-06CH11357. Portions of this work also were performed at the National Synchrotron Light Source (NSLS), Brookhaven National Laboratory. NSLS is supported by the U.S. Department of Energy, Office of Science, Office of Basic Energy Sciences, under Contract DE-AC02-98CH10886. NMR spectra were obtained with instrumentation supported by NSF CRIF:MU, CHE 0840401. We acknowledge the W.M. Keck Electron Microscopy Facility at the University of Delaware for the use of their JEOL JEM-2000FX and Tecnai-12 TEMs. We also thank E. Kelley for the synthesis of the PS homopolymer and Dr. K. Cavicchi for helpful discussions.

REFERENCES

(1) Lodge, T. P. *Macromol. Chem. Phys.* **2003**, *204*, 265−273.
(2) Phillip, W. A.; O'Neill, B.; Rodwogin, M.; Hillmyer, M. A.; Cussler, E. L. *ACS Appl. Mater. Interfaces* **2010**, *2*, 847−853.
(3) Lee, D. H.; Park, S.; Gu, W.; Russell, T. P. *ACS Nano* **2011**, *5*, 1207−1214.
(4) Hamley, I. W. *The Physics of Block Copolymers*; Oxford Science Publications: New York, 1998.
(5) Abetz, V.; Simon, P. F. *Adv. Polym. Sci.* **2005**, *189*, 125−212.
(6) Epps, T. H., III; Cochran, E. W.; Bailey, T. S.; Waletzko, R. S.; Hardy, C. M.; Bates, F. S. *Macromolecules* **2004**, *37*, 8325−8341.
(7) Bates, F. S.; Fredrickson, G. H. *Phys. Today* **1999**, *52*, 32−38.
(8) Meuler, A. J.; Hillmyer, M. A.; Bates, F. S. *Macromolecules* **2009**, *42*, 7221−7250.
(9) Kurt, A. K.; Matthew, T.; Frank, S. B.; Kristoffer, A.; Ralph, H. C. *J. Phys. II* **1992**, *2*, 1941−1959.
(10) Crossland, E. J. W.; Ludwigs, S.; Hillmyer, M. A.; Steiner, U. *Soft Matter* **2007**, *3*, 94−98.
(11) Crossland, E. J. W.; Kamperman, M.; Nedelcu, M.; Ducati, C.; Wiesner, U.; Smilgies, D. M.; Toombes, G. E. S.; Hillmyer, M. A.; Ludwigs, S.; Steiner, U.; Snaith, H. J. *Nano Lett.* **2008**, *9*, 2807−2812.
(12) Gobius du Sart, G.; Vukovic, I.; Vukovic, Z.; Polushkin, E.; Hiekkataipale, P.; Ruokolainen, J.; Loos, K.; Ten Brinke, G. *Macromol. Rapid Commun.* **2010**, *32*, 366−370.
(13) Bates, F. S. *Science* **1991**, *251*, 898−905.
(14) Bates, F. S.; Fredrickson, G. H. *Annu. Rev. Phys. Chem.* **1990**, *41*, 525−557.
(15) Epps, T. H., III; Bates, F. S. *Macromolecules* **2006**, *39*, 2676−2682.

(16) Matsen, M. W.; Bates, F. S. *J. Polym. Sci., Part B: Polym. Phys.* **1997**, *35*, 945−952.
(17) Lennon, E. M.; Katsov, K.; Fredrickson, G. H. *Phys. Rev. Lett.* **2008**, *101*, 138302/1−138302/4.
(18) Spontak, R. J.; Smith, S. D.; Ashraf, A. *Polymer* **1993**, *34*, 2233−2236.
(19) Feng, J.; Cavicchi, K. A.; Heinz, H. *ACS Nano* **2011**, *5*, 9413−9420.
(20) Urbas, A. M.; Maldovan, M.; DeRege, P.; Thomas, E. L. *Adv. Mater.* **2002**, *14*, 1850−1853.
(21) Lin, Y.; Daga, V. K.; Anderson, E. R.; Gido, S. P.; Watkins, J. J. *J. Am. Chem. Soc.* **2011**, *133*, 6513−6516.
(22) Daga, V. K.; Watkins, J. J. *Macromolecules* **2010**, *43*, 9990−9997.
(23) Daga, V. K.; Schwartz, E. L.; Chandler, C. M.; Lee, J.-K.; Lin, Y.; Ober, C. K.; Watkins, J. J. *Nano Lett.* **2011**, *11*, 1153−1160.
(24) Wang, J.-Y.; Chen, W.; Russell, T. P. *Macromolecules* **2008**, *41*, 4904−4907.
(25) Chen, J.; Frisbie, C. D.; Bates, F. S. *J. Phys. Chem. C* **2009**, *113*, 3903−3908.
(26) Ruzette, A.-V. G.; Soo, P. P.; Sadoway, D. R.; Mayes, A. M. *J. Electrochem. Soc.* **2001**, *148*, A537−A543.
(27) Young, W.-S.; Epps, T. H., III *Macromolecules* **2009**, *42*, 2672−2678.
(28) Young, W.-S.; Brigandi, P. J.; Epps, T. H., III. *Macromolecules* **2008**, *41*, 6276−6279.
(29) Wanakule, N. S.; Panday, A.; Mullin, S. A.; Gann, E.; Hexemer, A.; Balsara, N. P. *Macromolecules* **2009**, *42*, 5642−5651.
(30) Epps, T. H., III; Bailey, T. S.; Waletzko, R.; Bates, F. S. *Macromolecules* **2003**, *36*, 2873−2881.
(31) Gunkel, I.; Thurn-Albrecht, T. *Macromolecules* **2011**, *45*, 283−291.
(32) Simon, P. F. W.; Ulrich, R.; Spiess, H. W.; Wiesner, U. *Chem. Mater.* **2001**, *13*, 3464−3486.
(33) Tirumala, V. R.; Romang, A.; Agarwal, S.; Lin, E. K.; Watkins, J. J. *Adv. Mater.* **2008**, *20*, 1603−1608.
(34) Tirumala, V. R.; Daga, V.; Bosse, A. W.; Romang, A.; Ilavsky, J.; Lin, E. K.; Watkins, J. J. *Macromolecules* **2008**, *41*, 7978−7985.
(35) Chen, W.; Wang, J.-Y.; Wei, X.; Xu, J.; Balazs, A. C.; Matyjaszewski, K.; Russell, T. P. *Macromolecules* **2011**, *44*, 278−285.
(36) Wei, X.; Chen, W.; Chen, X.; Russell, T. P. *Macromolecules* **2010**, *43*, 6234−6236.
(37) Wei, X.; Li, L.; Kalish, J. P.; Chen, W.; Russell, T. P. *Macromolecules* **2011**, *44*, 4269−4275.
(38) Hashimoto, T.; Tanaka, H.; Hasegawa, H. *Macromolecules* **1990**, *23*, 4378−4386.
(39) Hashimoto, T.; Yamasaki, K.; Koizumi, S.; Hasegawa, H. *Macromolecules* **1993**, *26*, 2895−2904.
(40) Winey, K. I.; Thomas, E. L.; Fetters, L. J. *Macromolecules* **1991**, *24*, 6182−6188.
(41) Winey, K. I.; Thomas, E. L.; Fetters, L. J. *Macromolecules* **1992**, *25*, 2645−2650.
(42) Winey, K. I.; Thomas, E. L.; Fetters, L. J. *Macromolecules* **1992**, *25*, 422−428.
(43) Matsen, M. W. *Macromolecules* **1995**, *28*, 5765−5773.
(44) Matsen, M. W.; Bates, F. S. *Macromolecules* **1995**, *28*, 7298−7300.
(45) Floudas, G.; Hadjichristidis, N.; Stamm, M.; Likhtman, A. E.; Semenov, A. N. *J. Chem. Phys.* **1997**, *106*, 3318−3328.
(46) Huh, J.; Jo, W. H. *J. Chem. Phys.* **2002**, *117*, 9920−9926.
(47) Janert, P. K.; Schick, M. *Macromolecules* **1998**, *31*, 1109−1113.
(48) Likhtman, A. E.; Semenov, A. N. *Macromolecules* **1997**, *30*, 7273−7278.
(49) Bodycomb, J.; Yamaguchi, D.; Hashimoto, T. *Macromolecules* **2000**, *33*, 5187−5197.
(50) Epps, T. H., III; Chatterjee, J.; Bates, F. S. *Macromolecules* **2005**, *38*, 8775−8784.
(51) Tureau, M. S.; Rong, L.; Hsiao, B. S.; Epps, T. H., III *Macromolecules* **2010**, *43*, 9039−9048.
(52) Sugiyama, M.; Shefelbine, T. A.; Vigild, M. E.; Bates, F. S. *J. Phys. Chem. B* **2001**, *105*, 12448−12460.
(53) Tureau, M. S.; Epps, T. H., III *Macromol. Rapid Commun.* **2009**, *30*, 1751−1755.
(54) Allen, R. D.; Long, T. E.; McGrath, J. E. *Polym. Bull.* **1986**, *15*, 127−134.
(55) Varshney, S. K.; Jacobs, C.; Hautekeer, J. P.; Bayard, P.; Jerome, R.; Fayt, R.; Teyssie, P. *Macromolecules* **1991**, *24*, 4997−5000.
(56) Fetters, L. J.; Lohse, D. J.; Richter, D.; Witten, T. A.; Zirkel, A. *Macromolecules* **1994**, *27*, 4639−4647.
(57) Russell, T. P.; Hjelm, R. P.; Seeger, P. A. *Macromolecules* **1990**, *23*, 890−893.
(58) Tcherkasskaya, O.; Ni, S.; Winnik, M. A. *Macromolecules* **1996**, *29*, 610−616.
(59) Yang, J.; Lu, J.; Rharbi, Y.; Cao, L.; Winnik, M. A.; Zhang, Y.; Wiesner, U. B. *Macromolecules* **2003**, *36*, 4485−4491.
(60) Tyler, C. A.; Qin, J.; Bates, F. S.; Morse, D. C. *Macromolecules* **2007**, *40*, 4654−4668.
(61) Khandpur, A. K.; Foerster, S.; Bates, F. S.; Hamley, I. W.; Ryan, A. J.; Bras, W.; Almdal, K.; Mortensen, K. *Macromolecules* **1995**, *28*, 8796−8806.
(62) Lai, C.; Loo, Y.-L.; Register, R. A.; Adamson, D. H. *Macromolecules* **2005**, *38*, 7098−7104.
(63) Imai, M.; Saeki, A.; Teramoto, T.; Kawaguchi, A.; Nakaya, K.; Kato, T.; Ito, K. *J. Chem. Phys.* **2001**, *115*, 10525−10531.
(64) Mareau, V. H.; Akasaka, S.; Osaka, T.; Hasegawa, H. *Macromolecules* **2007**, *40*, 9032−9039.
(65) Meuler, A. J.; Ellison, C. J.; Evans, C. M.; Hillmyer, M. A.; Bates, F. S. *Macromolecules* **2007**, *40*, 7072−7074.